J. Materials, Conc. Struct., Pavements, JSCE, No. 571/V-36, 251-267, 1997 August

FAILURE ANALYSIS OF UNDERGROUND RC FRAME SUBJECTED TO SEISMIC ACTIONS

Xuehui AN[1] and Koichi MAEKAWA[2]

[1] Member of JSCE, Dr. of Eng., Seismic Eng. Dept., Tokyo Electric Power Services Co., Ltd. (Higashi-Ueno 3-3-3, Taito-ku, Tokyo 110, Japan)
[2] Member of JSCE, Dr. of Eng., Professor, Department of Civil Engineering, The University of Tokyo, (Hongo 7-3-1, Bunkyo-ku, Tokyo 113, Japan)

This paper presents failure analysis of underground RC frames. The Hanshin Great Earthquake in 1995 brought serious damage to RC frames for subway stations. For studying the collapse mechanism of underground RC, seismic response of a subway station is simulated in using FEM program WCOMD-SJ of two-dimension based on the path dependent RC smeared crack model, soil foundation and interfacial models. The shear failure of intermediate vertical columns is found to be the major cause of the structural collapse. Further, parametric study on reinforcement ratio and foundation properties is performed for investigating seismic resistant performance for underground RC culverts.

Key Words : *FEM, dynamic analysis, underground structure, RC, soil-structure interaction*

1. INTRODUCTION

Hanshin Great Earthquake on January 17,1995 brought about disastrous collapse of reinforced concrete structures including some underground subway stations in Kobe city. As catastrophic failure of underground structures was firstly experienced, it is much required to clarify the collapse mechanism of these underground frames and to update the latest seismic design if necessary.

In this study, underground RC frame with double decks for a subway station is targeted to study the failure mode and its mechanism, and to examine the computational tool for further study of earthquake resistant design. The observed damage reported in the literature[1),2)] is compared with analytical results for verification on which the enhanced seismic resistant design will be based in future.

2. COMPUTATION TOOL

In this paper, two dimensional FEM program WCOMD-SJ is used for analyzing coupled reinforced concrete and soil structures under seismic excitation. Here, the constitutive models for reinforced concrete, soil and the interface between soil and RC are installed.

In the model for reinforced concrete, the multi-directional smeared crack model of concrete is employed, and the constitutive law of reinforcing bars is composed. The concrete model consists of tension stiffening, compression and shear transfer models. These models are given as the relationship between average stress and average strain in reinforced concrete. The crack spacing, or density, and diameter of reinforcing bars have negligible effect on the spatially average stress-strain relation defined on RC control volume, as shown in **Fig.1a**[3),4)]. The continuum damage model of concrete encompasses the reduction of compressive capacity of cracked concrete in relation to the strain normal to the crack[5)].

A path-dependent constitutive model for soil is indispensable for dealing with kinematic interaction of RC-soil entire system under strong seismic loads, as shown in **Fig.1b**[6)]. Here, Ohsaki's model[7)] defines the formula for envelope to express the nonlinear relation of the shear stress-strain for soil as well as internal loop with Masing's rule. In addition, separation and sliding between soil and structure are taken into account along the interfacial zone as shown in **Fig.1c**.

The full path-dependent constitutive models were integrated in the scheme of Newmark step-by-step direct integration of both time and strain histories. In this way, the dynamic nonlinear response of RC-soil structure can be computed within the versatile computational scheme.

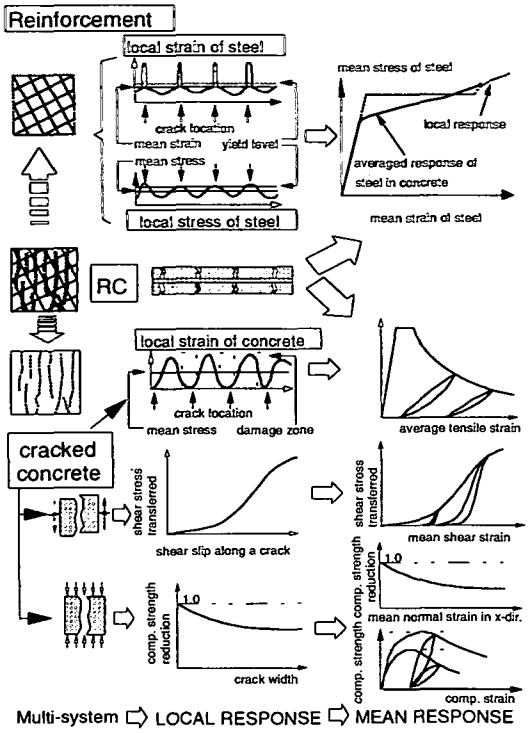

Fig.1a Constitutive model of reinforced concrete[3].

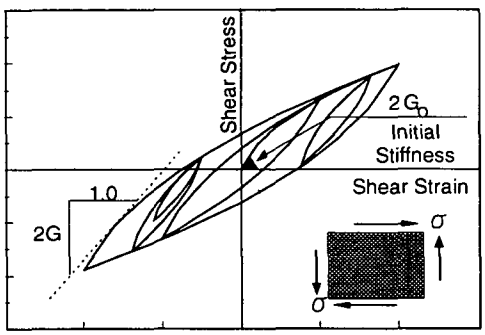

Fig.1b Computed shear stress-strain relation for soil[6].

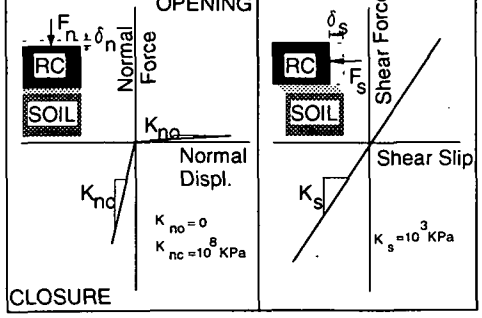

Fig.1c Normal and shear relations for RC/soil interface model[6].

3. COMPUTATION TARGET

One of the most typical damages experienced in Kobe in 1995 is the failure of intermediate columns in underground RC box culvert. Reported are 264 RC columns in the subway line. Among them, 139 columns were damaged and 118 of them were fatally collapsed. In this study, one typical section of a station is chosen for the collapse simulation and evaluation of seismic resistant performance. The scenario of failure and the final collapse of the structures are of great interest to the authors.

(1) Failure observation

Diagonal shear cracks were clearly observed in the intermediate columns of the station. Heavy damage was identified at the upper deck columns located at the middle of the underground frame spans, and subsidence occurred to the top slab as the column could not carry the dead load after shear failure occurred (**Fig.2a**). The maximum of subsidence reached 5cm by observation. But for the lower deck columns, the damage was not so serious as to finally fail. Only few diagonal shear cracks in the column were seen (**Fig. 2b**). The typical failure of this RC structure is the collapse of intermediate columns accompanying shear cracks and the damage concentrated into the upstairs columns of the double deck frames.

(2) Layout and structural details

Fig.3a gives the shape and dimension of the station section consisting of RC members[1),2)]. There are two floors in this RC box type culvert and in each floor one RC column was placed. For this section, the spacing of columns is 5m. The RC underground culvert has an outer dimension of 16.68m width and 13.25m height. The wall thickness is 0.8m in the first floor and 1.0m in the second floor. The thickness of the top slab is 1.0m and 1.3m for the bottom slab. The thickness of middle slab is 0.6m. The intermediate column has a cross section of 0.7m x 1.4m for the upper level and 0.6m x 1.5m for lower level with average reinforcement ratio 6.0%. The columns are idealized being completely fixed to the slabs both in reality and in computation. The station is inside the earth with 5m overlay of soil. The underground system for dynamic simulation is composed of both the 2D RC frame and the surrounding soil.

Fig.3b shows reinforcement arrangement of the station section concerned. The intermediate columns, which suffered from serious damage in the earthquake, has the features of reinforcement arrangement as heavily reinforced in the longitudinal direction and few web reinforcement placed. The longitudinal reinforcement ratio is 5.1% for the upper

Fig.2a Collapse of a column at the upper level.

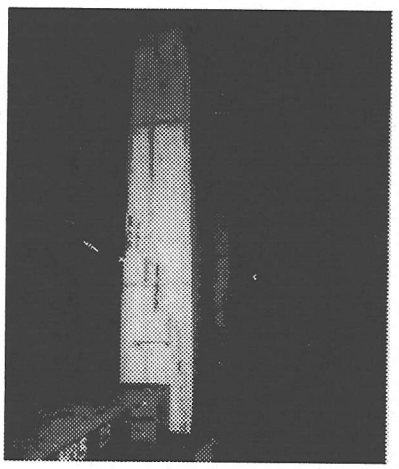

Fig.2b Shear cracks of a column at the lower level.

column and 5.7% for the lower column. The web reinforcement ratio is only 0.075%–0.15%. This amount can not substantially serve as shear reinforcement. **Fig.5** and **Table 1** show the details of the surrounding soil layers. In the computation, the acceleration seismic wave was applied at the base of layer 6 as the stiffness of layer 7 is assumed large enough to be regarded as a rigid engineering boundary for computation.

(3) Input ground acceleration waves

Earthquake motions that are used for input were recorded at Kobe meteorological observatory and other sites as shown in **Fig.4** and **Fig.29** in the later section. Both horizontal and vertical acceleration records are used for simulating dynamic response of soil-RC box system having longer dimension along an axis of subway line. It must be noted that used

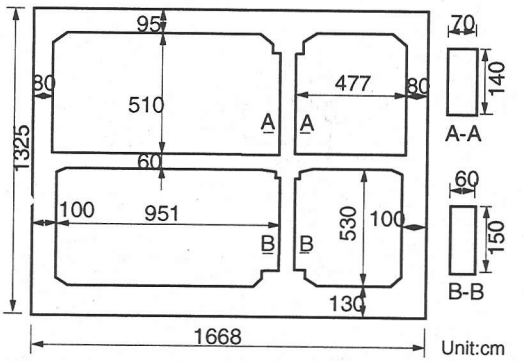

(Space of columns = 5m)

Fig.3a Dimension of the target RC frame.

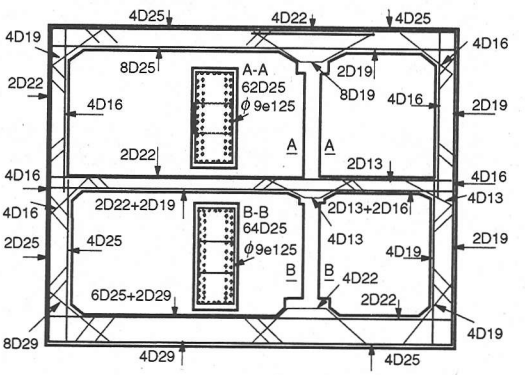

(Steel bar number /m)

Fig.3b Reinforcement arrangement of the target RC frame.

seismic actions are not the most expected inputs on the foundation rock but mere records measured on the ground surfaces as a result of magnification by the effect of propagation path of soil foundation.

Since the authors' capability is so limited as to produce the most reliable seismicity at the construction site, magnified ground surface waves are used as a substitute of the base rock accelerogram. It means difficulty to investigate the real cause of disaster which actually occurred. But, it may be possible to investigate the intrinsic structural performances under severe seismic actions and to examine applicability of coupled structural failure analysis and soil foundation. Then, this paper is directed in a great deal to structural aspects and check of computational capability. As a future stage, joint works with seismic field of study should follow this structural oriented investigation here.

For seismic performance check of existing structures, most expected seismic actions and material properties already developed should be defined since the purpose of verification is directed to actually attained performances.

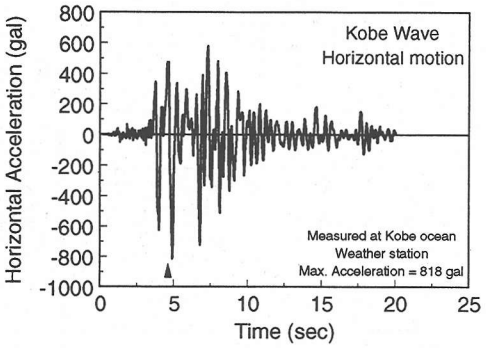

Fig.4a Horizontal acceleration of earthquake wave used.

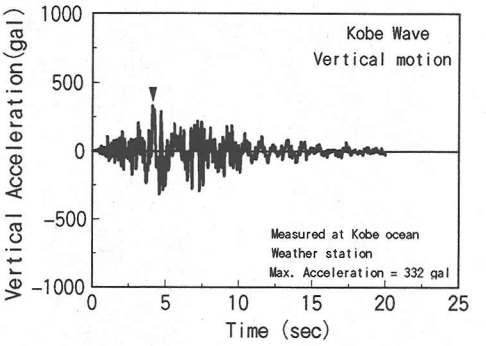

Fig.4b Vertical accceleration of earthquake wave used.

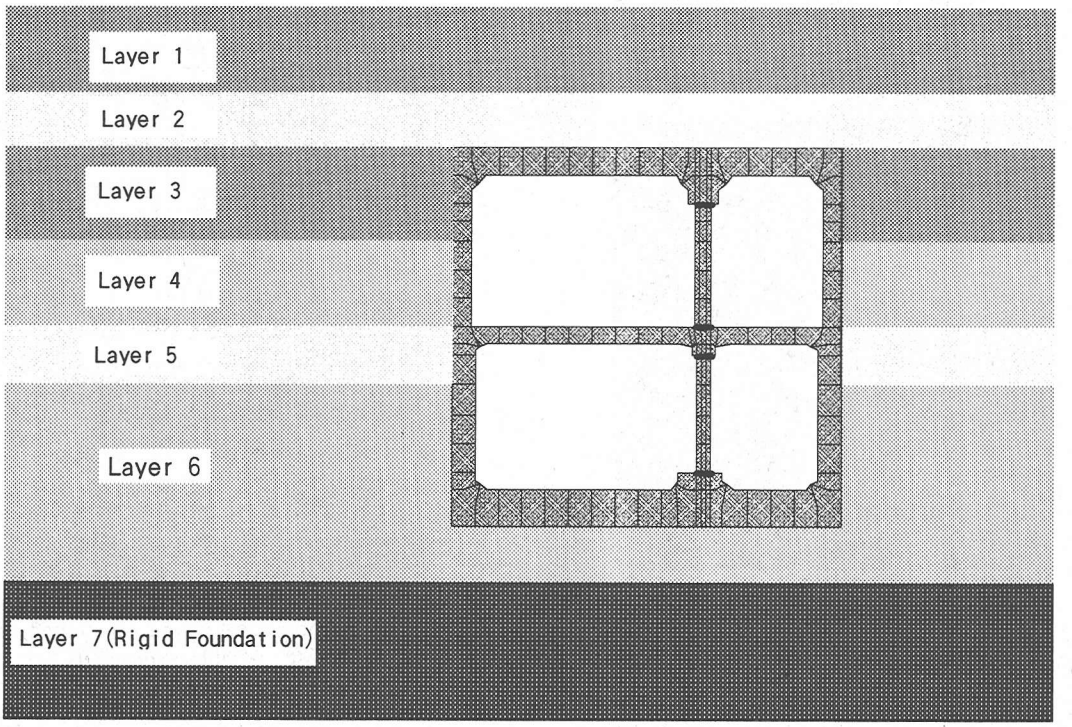

Fig.5 Soil profile of surrounding foundation.

Table 1 Characteristic variation of surrounding soils.

	Layer 1	Layer 2	Layer 3	Layer 4	Layer 5	Layer 6	Layer 7
Layer thickness(m)	3.0	2.0	3.25	3.0	2.0	7.0	>10.0
SPT-N	10	18	20	15	30	42	50
Vs (m/s)	205.0	246.0	256.6	228.7	301	345.3	410.7
Gs (kgf/cm^2)	757.1	1212	1318	1047	1823	2386	2840
Es (kgf/cm^2)	2196	3514	3822	3037	5288	6921	8240
Weight density (t/m^3)	1.8	2.0	2.0	2.0	2.0	2.0	2.0
Soil Type	clay	sand	clay	sand	clay	clay	clay

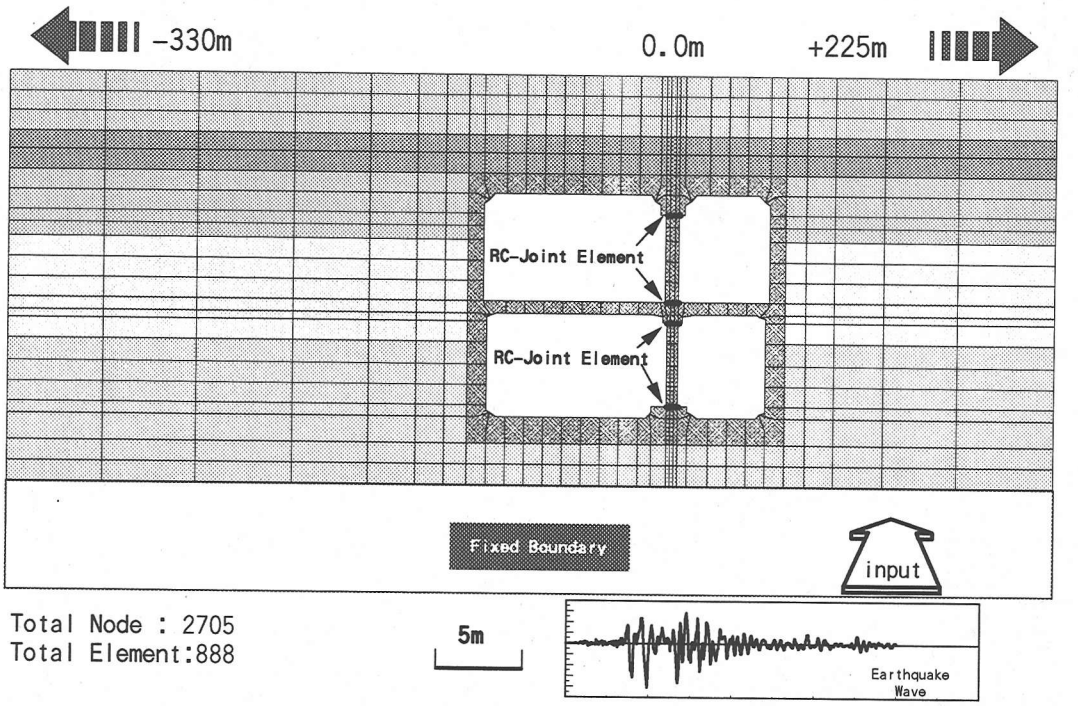

Fig.6 Central part of the finite element mesh of soil-RC used in FEM analysis.

(4) FEM mesh for RC frame and foundation

The finite element discretization is shown in **Fig.5,6**. Higher order isoparametric elements are used to analyze the target section. In flexure, only one layer of higher order elements is necessary and sufficient but in shear, several layers are required since shear strain develops nonlinearly over the thickness of members unlike flexural normal strains[8]. Then, three layers are placed at the intermediate columns and mesh sensitivity and convergence were checked in advance. As the thickness of RC outer frame and the column are different, the stiffness changes sharply near the joint plane. In order to account for the incontinuous deformation rooted in the joint area, RC joint elements are placed between the column and slab. The two extreme sides of this whole analysis domain have the mixed artificial boundary elements to simulate the far field of soil layers[8].

4. COLLAPSE SIMULATION OF SUBWAY STATION

The computation of coupled underground RC and the surrounding soil system under Kobe earthquake wave was conducted by **WCOMD-SJ**[3]. The following results give the behavior of the system under seismic load and the induced forces to the intermediate column.

(1) Inelasticity of the whole RC structure[8]

In order to indicate the damage level of the entire RC structure in terms of leakage resistance against ground water after earthquake, crack width oriented inelastic output in time domain is needed. The first strain invariant denoted by (I_1) is closely associated with the crack occurrence and expansion of the in-plane element (volumetric change of the element)[8]. The mean strain invariant denoted by (I) can be defined as the spatial average value of (I_1) for all RC elements. The value is equal to zero in the case of elastic shear behavior as no volumetric change and no residual deformation exist under pure elastic shear deformation. Hence the mean strain invariant (I), called as inelastic strain, can be adopted to represent the magnitude of the damage of reinforced concrete. The value of (I) can be calculated as follows.

$$I = \sum_{allelements} I_1(x,y)dx \cdot dy / A, \quad I_1 = \frac{\varepsilon_1 + \varepsilon_2}{2} \qquad (1)$$

where, ε_1 and ε_2 are the 2-D principal strains at (x,y) and A is the total area of the RC in-plane elements.

Fig.7 shows the inelastic strain (I) of the target RC frames in time domain. This index is used to qualitatively present how much damage to the RC structure and how much deformation resided after the dynamic action. In this figure, we can see great

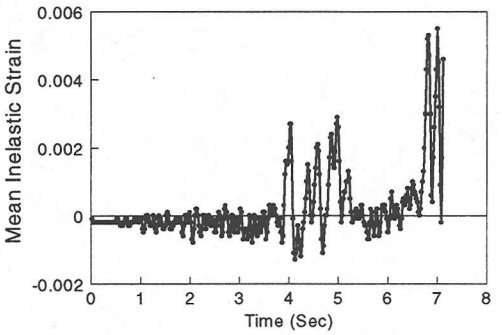

Fig.7 Inelastic strain representing damage of RC in time domain.

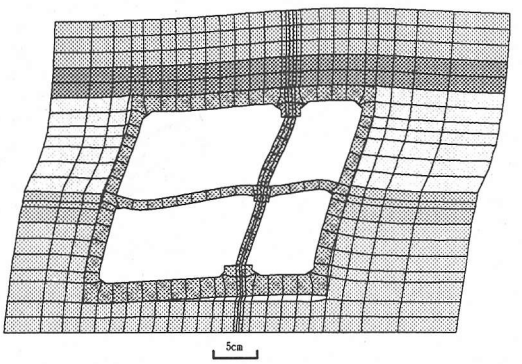

Fig.8a Deformation profile of RC-soil system just before failure.

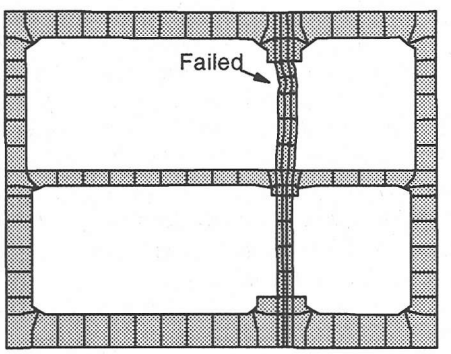

Fig.8b Deformation profile of station at failure.

increase in the inelastic strain at 7.32 sec and the structure reached failure.

(2) Dynamic response of the underground RC

Fig.8a gives the magnified deformation profile of the RC-soil system at the maximum response just before the failure of RC in shear. The maximum deformation at the top column is about 0.6% by average shear. And **Fig.8b** shows the deformational profile of the station at the failure. It can be seen that the deformation is concentrated into the upper intermediate column, which was the actual failure location of the entire RC structural system.

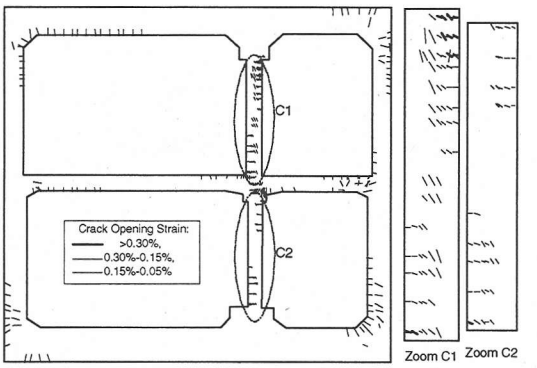

Fig9a Crack pattern of structure just before failure.

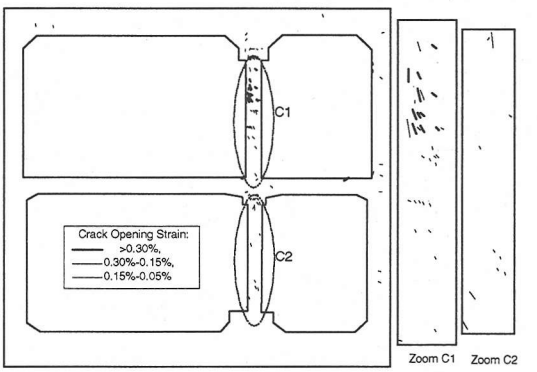

Fig.9b Cracks developed at the failure.

(3) Crack pattern of the RC frame

In order to confirm the location of failure and the failure mode, the crack pattern of the structure just before the failure is shown in **Fig.9a**, and **Fig.9b** indicates the cracks which are propagating during the failure process. From **Fig.9a** it can be seen that the large cracks are concentrated into the upper column, on the contrary, the lower column and the other parts of the frame have just small cracks. All cracks shown in **Fig.9b** occur in the last step of failure. We can see very clearly that only large shear cracks developed in the upper column, crossed the section of this column and caused the failure. These crack patterns with the observed cracks shown in **Fig.2** look fairly realistic.

(4) Internal stresses in the intermediate column

Computational results and observation show that the major collapse may occur at the intermediate column. It is important to discuss the induced forces and ductility of the internal columns. **Fig.10** shows the internal nominal stresses (axial compression and shear divided by the cross-sectional area of members) and the ductility of the column for both upper and lower parts.

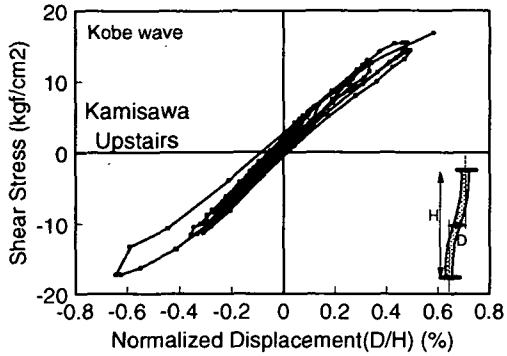

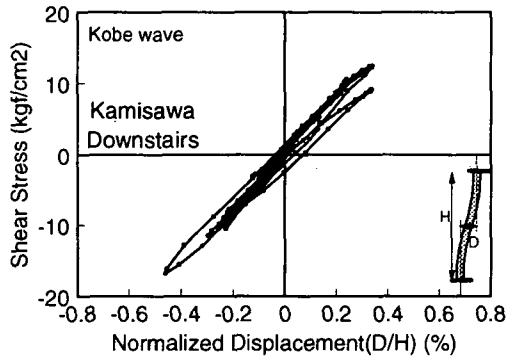

Fig10a Shear stress-displacement relationship for columns.

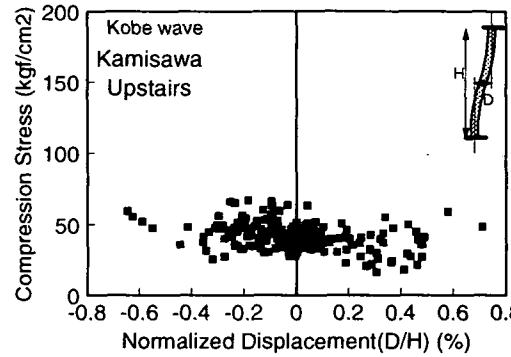

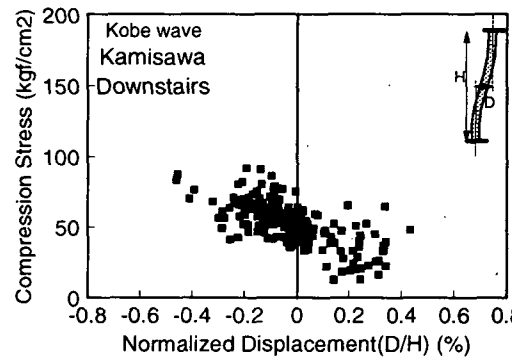

Fig.10b Compression stress variation of the columns.

Fig.10a shows the relation between the nominal shear stress (shear force normalized by the cross-sectional area of a member) and the relative displacement between top and bottom of the column. The relative displacement is also normalized by the height of the column. The column fails with the maximum normalized displacement 0.7% and maximum shear stress 18kgf/cm^2. The lower column undertakes similar nominal stress with slightly smaller shear displacement and no failure takes place.

Fig.10b shows the variation of nominal compressive stress in the columns. It can be seen that the compressive stress varies between 20kgf/cm^2 and 70 kgf/cm^2 due to the up and down motion of the earthquake. The maximum compressive stress is less than 100kgf/cm^2 and far away from the compression capacity of the RC columns.

(5) Collapse mechanism study

According to FEM simulation of the failure mechanism, it is considered that the RC column would lose axial load carrying capacity after the occurrence of the localized diagonal shear cracks, and sudden failure of the outer frame would be followed. Some cracks would be introduced at the lower column and the corner of the RC box but with lower damage level.

The aim of dynamic analysis of the RC underground structure is to study the rational seismic resistant design method based on the knowledge of the collapse mechanism investigated. As most of the damage of underground RC is rooted in the diagonal shear failure of the intermediate column[9], the shear behavior of the RC columns will be checked with the shear capacity equation of the JSCE code[10] as,

$$V_c = V_{cd} + V_{sd} \tag{2}$$

where, V_c is the shear capacity of the RC member; V_{cd} is the shear force carried by concrete and longitudinal reinforcement; V_{sd} is the shear force carried by the web reinforcement. V_{cd} and V_{sd} can be evaluated by the following formulas.

$$V_{cd} \propto (\rho_l)^{\frac{1}{3}} (f_c')^{\frac{1}{3}} (d)^{-\frac{1}{4}}$$

$$V_{sd} \propto \rho_w \tag{3}$$

where, ρ_l is the reinforcement ratio of longitudinal bars; ρ_w is the reinforcement ratio of web steel; f_c' is the compressive strength of concrete and d is the effective depth of RC member.

From these equations, the shear capacity of the upper column in underground RC can be calculated. If no axial force is considered, the shear strength of this column is 14.6kgf/cm^2. As the compression force

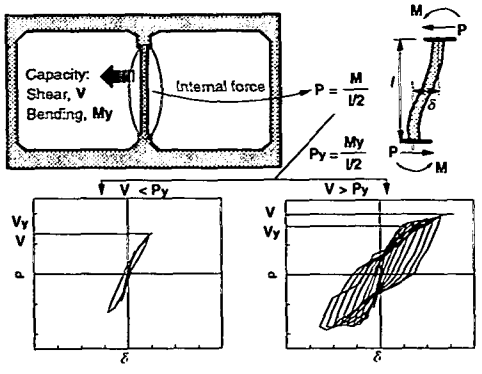

Fig. 11 Interaction of shear capacity and ductility.

varied from 10kgf/cm^2 to 100kgf/cm^2 in the dynamic response, the shear capacity reaches 17.2kgf/cm^2 as the maximum value in considering the axial compression force. The FEM computation above shows that shear stress in the upper column can reach 18kgf/cm^2, a little bit higher than the shear strength.

Another aspect to evaluate the seismic resistant capacity of the RC member is the ductility level. In order to avoid the sudden failure, the RC member should be designed to fail after yielding of longitudinal reinforcement. In the dynamic simulation of the underground RC, it was found that the intermediate column failed before or just after yielding of longitudinal bars. This was also pointed out by some 3-D FEM analysis[9]. So it is necessary to discuss the ductility of the column in RC frames.

The ductility level of RC member can be estimated by,

$$\frac{V_c}{V_y} \geq N = N_{rq} \tag{4}$$

where, N is a factor which influences the ductility of the RC member. If N is less than unity, the member behaves with brittle mode of failure. V_y is the shear force corresponding to the bending capacity denoted by M_y (**Fig.11**), and if defined as yielding shear force herein. Then, V_y can be calculated as,

$$V_y = \frac{My}{H/2} \propto \rho_l \tag{5}$$

where, H is the height of the column.

In the case of upper column of the underground RC concerned, the bending capacity is more than 410 ton-m when yielding of longitudinal bars takes place. The shear force at this time is about 20kgf/cm^2. Then, ductility factor N is 0.73, which is much smaller than unity. Certainly, the intermediate column ductility is less accompanying diagonal shear cracking.

For evaluating the seismic resistance, both the shear capacity and the ductility should be considered. From **Eq.(2)**, it seems that for RC member with ordinary concrete strength, there are two ways to increase the shear capacity, one is to increase the amount of longitudinal reinforcing bars, another one is to enhance the web reinforcement (See **Fig.11**).

In the first case, the bending capacity, defined as M_y will be simultaneously increased. As the bending capacity is corresponding to the yielding of main reinforcing bars, the shear force V_y at the yielding moment becomes very large, as calculated by **Eq.(5)**. The shear capacity will also be increased according to the JSCE code as,

$$V_c \propto (p_l)^{\frac{1}{3}} \tag{6}$$

According to **Eq.(5)** and **Eq.(6)**, the yielding shear force increases more than the shear capacity as the amount of main reinforcement rises in general. RC members with this kind of reinforcement arrangement are very brittle, and fail suddenly without much ductility. The failure of the intermediate columns of the subway stations is categorized into this case.

On the other hand, if the shear capacity is increased by enhancing the web reinforcement, the shear capacity V can be larger than the yielding shear force V_y. Then the ductility of the RC member will be elevated. RC members having higher shear capacity generally have higher seismic resistant performance.

5. ENHANCEMENT OF RC SEISMIC PERFORMANCE

As discussed above, the shear capacity level of the existing column in the underground RC is found to be lower and results in the small ductility. In order to enhance seismic resistance of RC structures in general, both shear capacity and ductility are effective.

But, the capacity of intermediate columns of underground box sections hardly influence on the overall shear deformation of RC and the induced sectional forces, because the structural deformation is much associated with that of interacting soil foundation. Since the chief required performance of the column is to sustain vertical forces no matter how large the shear deformation of the box section is induced. For underground RC structures, the member ductility is much to be focused in design of newly constructed structures and retrofitting of existing RC. Then, the ratio of shear capacity to the flexure will be of great interest to us.

(1) Increase in web reinforcement ratio in the intermediate column

Computation is based on the same RC frame as that in the previous chapter. The web amount in the

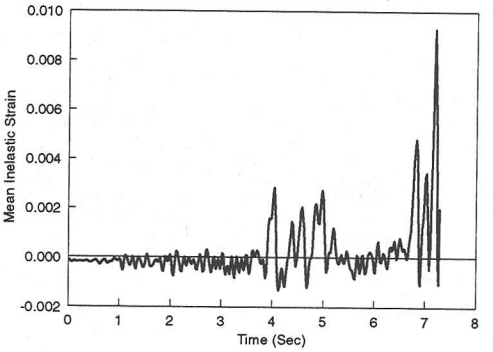

Fig.12 Inelastic strain representing damage in time domain.

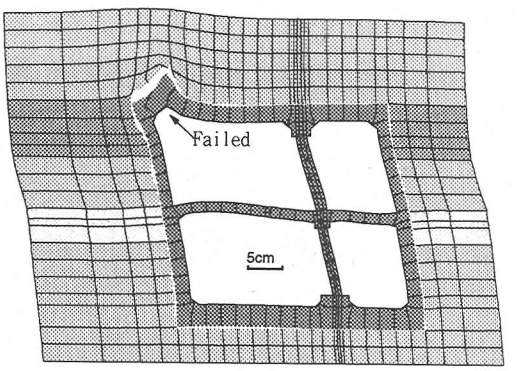

Fig.13 Deformation profile of RC-soil system at failure.

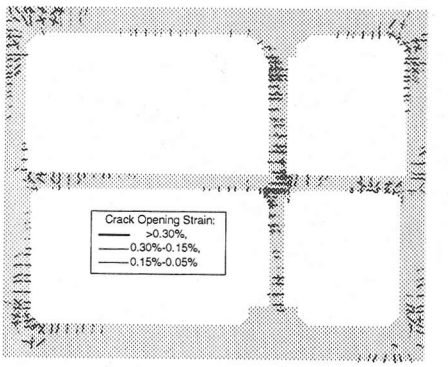

Fig.14a Crack pattern of structure just before failure.

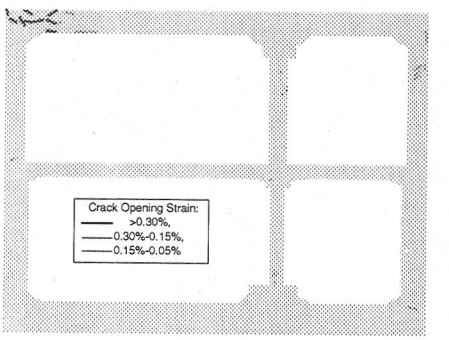

Fig.14b Cracks developed at the failure.

column is increased up to 0.76% (D16 with spacing of 7.5cm, volumetric ratio is 1.66%) , and the shear capacity can reach 33.3kgf/cm^2 according to the shear equation of JSCE code (no consideration of axial compressive force). As no change is made in longitudinal reinforcement arrangement, the yielding shear force V_y is still 20kgf/cm^2. The shear to flexure capacity ratio N is 1.67. In this case, the columns are expected to have sufficient shear resistance against seismic actions.

a) Inelasticity of the whole RC structure

Fig.12 shows the inelastic strain *(I)* of shear enhanced case with additional web reinforcement in time domain. In this figure, we can see that the structure fails at 7.32 second.

b) Dynamic response of the RC frame

Fig.13 shows the deformational profile of the station at the failure. It can be seen that the deformation is concentrated at the corner of the RC outer frame, and the failure took place at the upper slab. Since the number of finite element layer is just one, failure possibility will be again checked in terms of shear forces developed and empirical formula by the JSCE code. There is no localization of deformation in the columns, since the intermediate column is strongly reinforced in shear.

c) Crack pattern of the RC frame

For identifying the failure location and the failure mode when the web of the column is much reinforced in shear, **Fig.14a** shows the crack pattern of the structure just before the failure. In **Fig.14a** large cracks are seen in several places such as the upper column, the lower column, the middle slab-column joint and the corners of the frame. **Fig.14b** shows the cracks which developed at the failure. All the cracks shown in **Fig.14b** are introduced in the last step of computation. We can see just distinct shear cracks within the upper slab, near the left corner, crossing the section of this column. So the shear is brought about at the upper slab near the corner.

d) Internal stresses in the intermediate column

The computational results of the shear enhanced case indicate that the collapse takes place not at the intermediate column but at the upper slab near the left corner. Discussion of induced forces in the internal column may be advisable for further clarifying failure section in the slab.

Fig.15 shows the relation between the nominal shear stress and the relative shear displacement of the upper and lower columns. The relative displacement is normalized by the height of the column. For the upper column, when the failure occurs, the shear stress in the column is small. The maximum

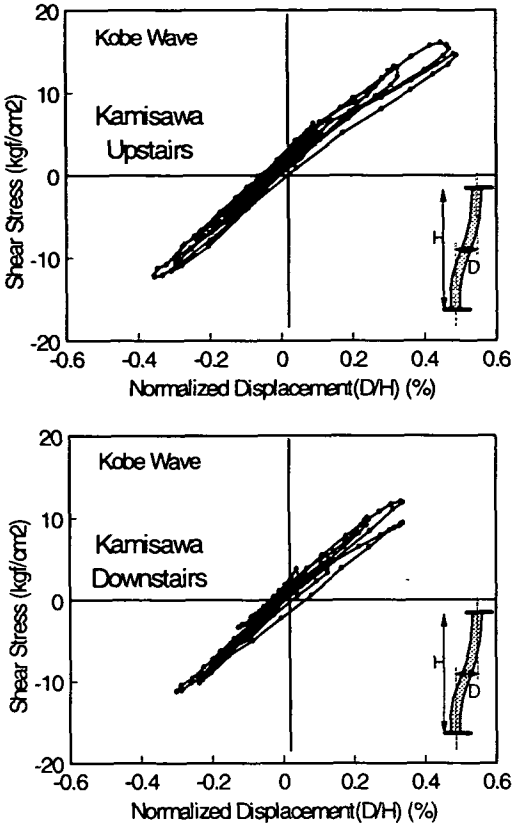

Fig.15 Shear stress-displacement relationship for columns.

normalized displacement is 0.5% and the maximum shear stress is 18kgf/cm^2.

On the other hand, the lower column experiences shear stress of 12kgf/cm^2 and no failure takes place. There exists less difference of **Fig.10a** and **Fig.15**, but quite much difference in failure mode. The shear capacity is much increased in this case, but the ductility response remains unchanged as the main reinforcement is kept constant and absolutely large.

e) Internal stresses in the slab corner

Fig.16 shows the variation of shear stress in the section of the corner. It can be seen that the shear stress reaches 18kgf/cm^2 just before failure. The estimated shear capacity of this slab in use of JSCE code[10] is 15.2kgf/cm^2. So, the slab is supposed to fail in shear.

f) Collapse mechanism of the subway station

In the shear enhanced case, according to FEM simulation, it is considered that the intermediate RC column gets strong enough to resist the shear and will not fail under the earthquake wave. But, the overall structural performance is not improved much as the main reinforcement ratio is kept unchanged. Then, the partial strengthening merely results in the shift of the weakest section.

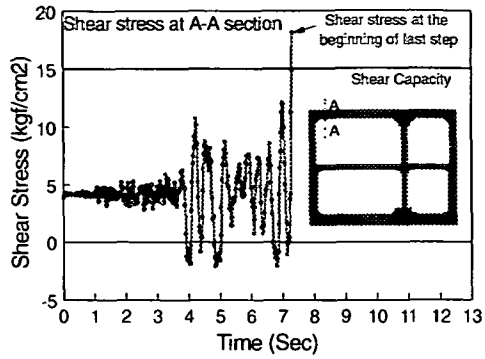

Fig.16 shear stress variation at the failure section.

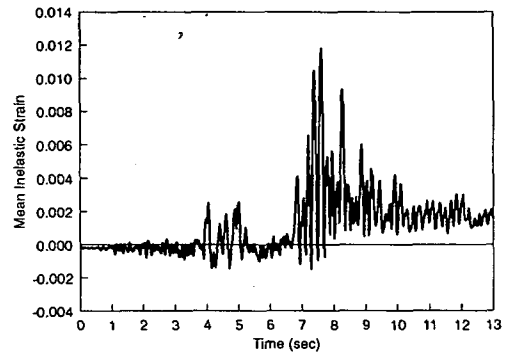

Fig.17 Inelastic strain representing damage in time domain.

(2) Reduction of main reinforcement for improving ductility

The computation was conducted based on the same RC frame in which web reinforcement ratio in the column is increased up to 0.76%, which is the same as that of section (1). But the longitudinal reinforcement ratio reaches 3.67%, trying to enhance the ductility of the column. The shear capacity comes up to 32.1kgf/cm^2 according to the JSCE code. The main reinforcement ratio is reduced so as to get the yield shear stress as 14.4kgf/cm^2 equivalent to yield of main steel. The shear/flexure capacity ratio N can reach 2.23 in this case. Thus, much ductility is granted with sufficient shear capacity.

a) Inelasticity of the whole RC structure

Fig.17 shows the inelastic strain (I) of the enhanced shear and reduced flexure case in time domain. Herein, we can see that the structure does not fail until the seismic load leaves.

b) Internal stresses in the intermediate column

It can be seen more clearly by comparing the induced forces in the internal column and the failure section in the slab with the web enhanced case discussed in the previous section.

Fig.18 shows the relation between the nominal shear stress and the relative displacement. The relative displacement is normalized by the height of

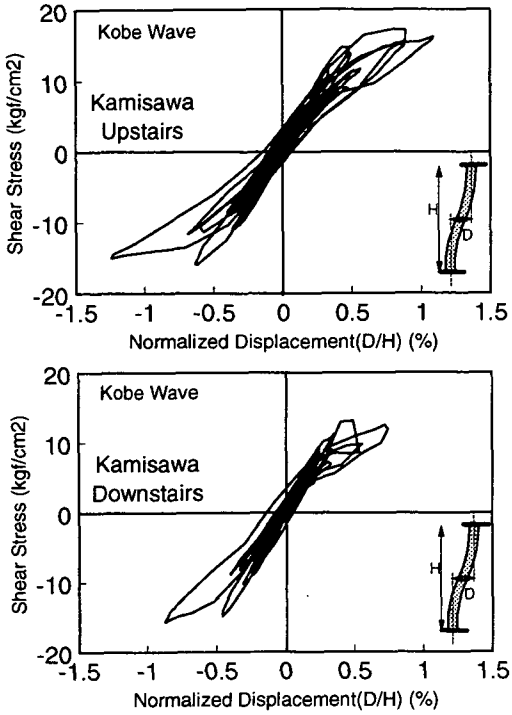

Fig.18 Shear stress-displacement relationship for columns.

the column. For the upper column, the maximum normalized displacement can reach 1.2% and the maximum shear stress does 18kgf/cm^2. On the other hand, the lower column undertakes shear stress as 12kgf/cm^2. Through the comparison of this figure with **Fig.11a** and **Fig.15**, the improved ductility accompanying the flexural nonlinearity is clearly identified.

c) Internal stresses in the slab corner

In order to compare this high ductility case with previous one, the variation of shear stress in the section of corner, where the failure took place in the enhanced shear with just additional web reinforcement case is shown in **Fig.19**. The maximum shear stress is reduced down to 15kgf/cm^2 by reducing the flexure capacity but elevating the ductility of the structure.

(3) Summary of the parametric computation

The parametric computation of three cases is summarized in **Table 2**. These trial computations show that both the shear capacity and the ductility are important factors for seismic resistant performance. The RC member with low shear strength will fail in shear mode under seismic load, and the RC structure with higher shear strength and ductility can survive during the earthquake. It can be found from the computational experience that the ductile structure possesses higher seismic resistance.

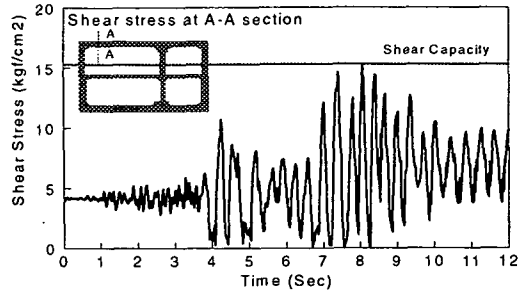

Fig.19 Shear stress variation at the corner section.

Table 2 Parametric study on member ductility

Case	Original	Enhanced web	Enhanced web + reduced flexural
Ratio of main bar	5.1%	5.1%	3.67%
Ratio of web	0.15%	0.76%	0.76%
V (kgf/cm^2)	14.6	33.3	32.1
V_c (kgf/cm^2)	10.0	10.0	8.8
V_s (kgf/cm^2)	4.6	23.3	23.3
V_y (kgf/cm^2)	20	20	14.4
N	0.73	1.67	2.23
Failure location	upper column	upper slab	no failure

6. SOIL STRUCTURE AND SEISMIC ACTIONS

The dynamic system discussed above includes the underground RC and soil foundation. The change of reinforcement ratio in the RC frame was proved to be very effective from a view point of the damage control. In this section, interacting aspects with soil foundation and the wave property will be studied for further understanding of the behavior of whole dynamic system.

(1) Soil profile

In the original case for Kamisawa station, the soil foundation property varies in the vertical direction. The shear modulus of soil is specified larger as the depth increased. **Fig. 20** shows the soil profile used as original. The soil around the upper deck is softer than the one around the lower deck. As the softer soil may cause larger induced shear deformation in the RC culvert, larger shear deformation is supposed to be produced in the upper column under the earthquake. This may be the reason why the column of the upper floor failed but the column of the lower floor had just few shear cracks.

The effect of soil profile can be checked by intentionally changing the soil profile in the computation. If the failure mode and position would be affected by the change of soil profile, soil structure would be found to have much to do with the failure

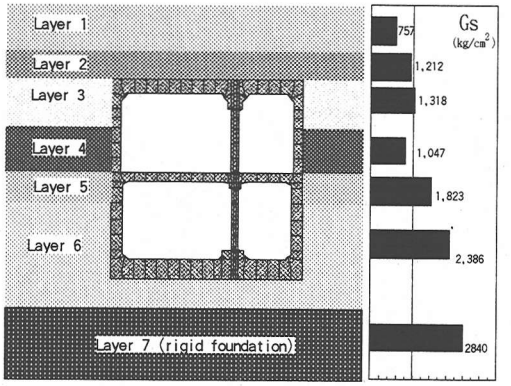

Fig.20 Assumed shear modulus profile for soil foundation.

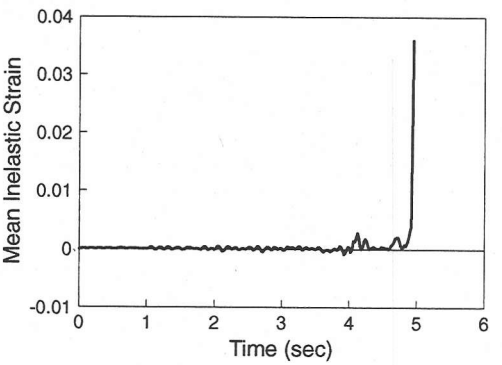

Fig.21 Inelastic strain representing damage in time domain.

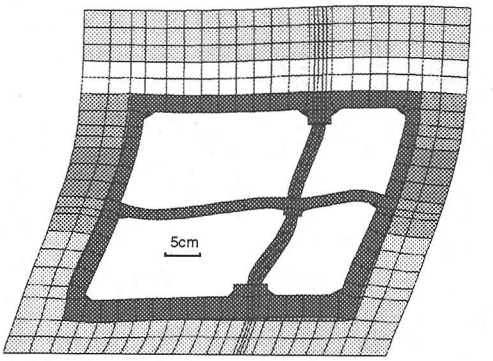

Fig.22a Deformation profile of RC -soil system just before failure.

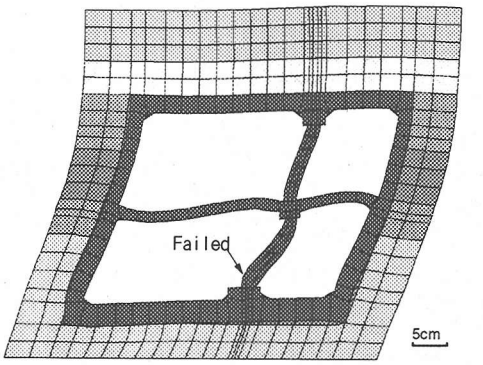

Fig.22b Deformation profile of station at failure.

mechanism. For this purpose, the computation is performed with the different soil profile from the standard, that is, the foundation around the RC frame is taken as the same material property of the shear modulus of 1318 kgf/cm^2, which is similar to that of layer 3 in the original case. Other factors are kept the same as the original one.

The computational results of this modified soil profile are shown in **Fig.21--Fig.24**. The inelastic strain of the RC box in time domain is shown in **Fig.21**. By comparing **Fig.21** with the original case (**Fig.7**), much difference of the response is identical. The structure failed at 5.2 sec with abrupt increase in the structural damage. As the mean shear modulus of the original case is 1603 kgf/cm^2, the premature failure would be associated with soft foundation.

The next point of interest is the location of failure. **Fig.22** shows the deformation profile of the RC frame under the dynamic excitation. In **Fig.22a**, which shows the deformation profile just before failure, larger deformation at the lower column is seen than the original case (**Fig.8a**). In order to focus on the failure position more clearly, the deformation profile of the station at failure is shown in **Fig.22b**. The deformation is concentrated in the lower column. It means the failure position changes from upper to lower as the soil profile be changed as uniform.

The crack pattern shown in **Fig.23a** supports the above stated discussion on the failure location. There are many cracks in the two columns, unlike the case in **Fig.9**. The damage is much heavier than that in the original case (**Fig.9a**). **Fig.23b** shows cracks developing in the last step. The diagonal shear failure and cracking are sharply detected.

Fig.24 shows the internal shear stresses and the shear deformation of the column for both upper and lower parts of the frames. The great shear deformation is produced in the lower column which finally failed. The shear stress is also higher in the lower column than that in the upper one.

All these computational results make it clear that the soil profile will affect the damage occurring in the RC underground structure. It also proves that the soft foundation around the upper deck of the frame is one of the main reasons why upstairs columns are damaged in reality. Regarding the magnitude of shear deformation in soil-RC coupled systems, combination of wave characteristics, structural and soil stiffness is a point of design. As has being well pointed out, the entire system has to be modeled in seismic design of underground structures.

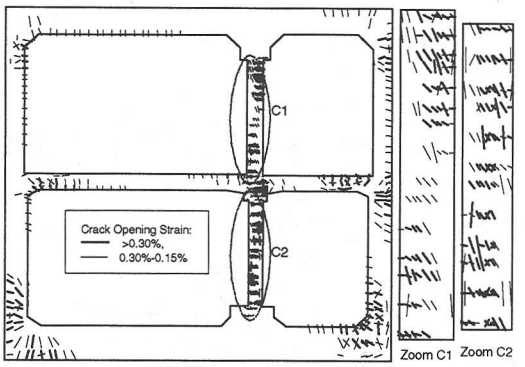

Fig.23a Crack pattern of the RC frame just before failure.

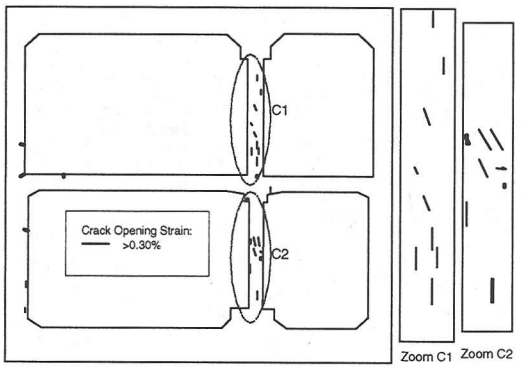

Fig.23b Cracks produced at the failure.

(2) Effect of vertical seismic action

One of the characteristics of the seismic motion used in the above discussion is that the vertical component of the ground motion is rather high. In fact, the maximum vertical acceleration reached about 40% of the maximum horizontal one. In general, the vertical component of seismicity is ignored in some cases owing to its small contribution to the structural safety and dynamic response. However, influenced structural behavior was reported[11] even when the vertical ground motion is perfectly cut off in the dynamic computation. So it is meaningful to discuss the influence of the vertical ground motion, especially for the case where failure does not occur in the column.

In section 5.1 the case where the column is heavily reinforced in shear was discussed and the failure took place in the upper slab. Here, the computation will be done for this case while the vertical component of the ground motion is completely cut off.

Computed results under no vertical seismicity are summarized in **Fig.25--Fig.28**. **Fig.25** shows the inelastic strain in time. The structure failed at 6.96 second.

In order to identify the failure position more clearly, the deformation profile at failure is shown in

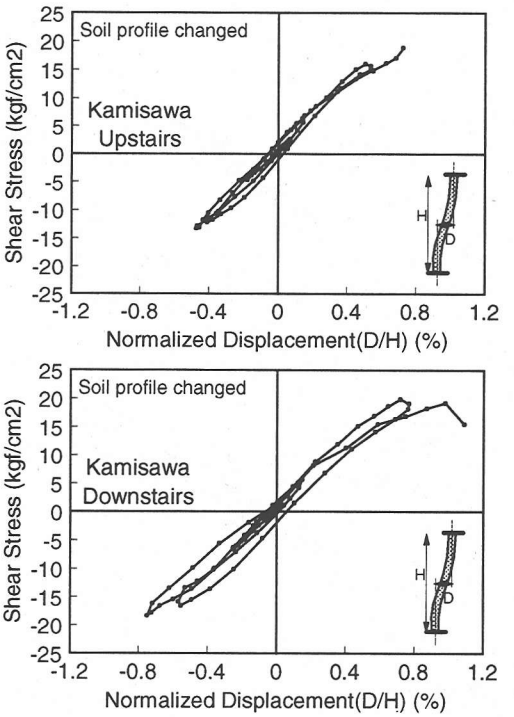

Fig.24 Shear stress-displacement relationship for columns.

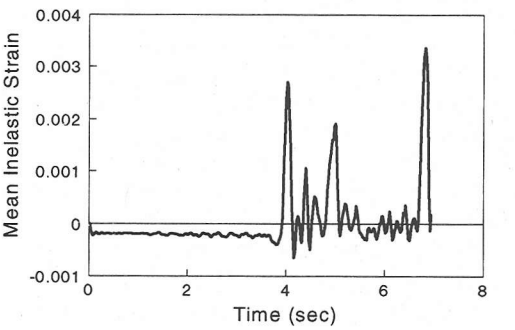

Fig.25 Inelastic strain representing damage in time domain.

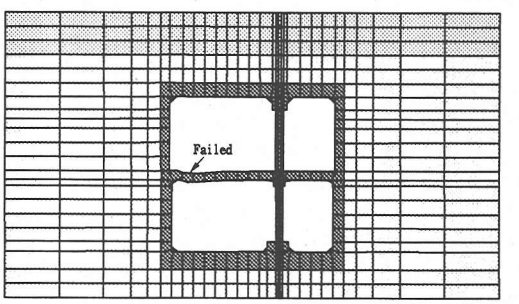

Fig.26 Deformation profile of station at failure.

Fig.26. It can be seen that the deformation is localized in the left side of the middle slab. It means the failure position shifts from the upper slab to the middle slab owing to avoidance of the vertical component of the ground motion.

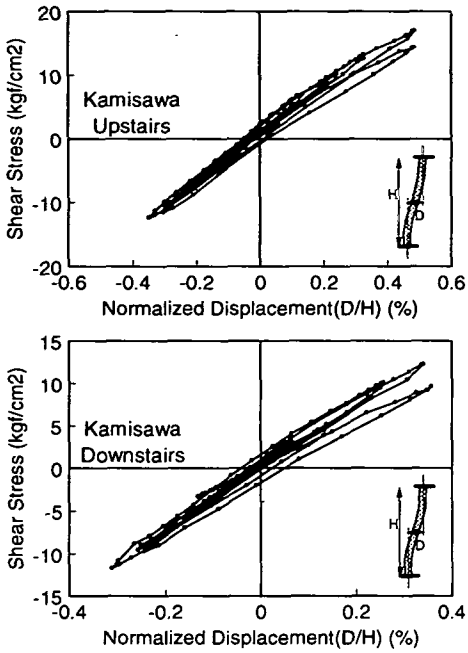

Fig.27 Shear stress-displacement relationship for columns.

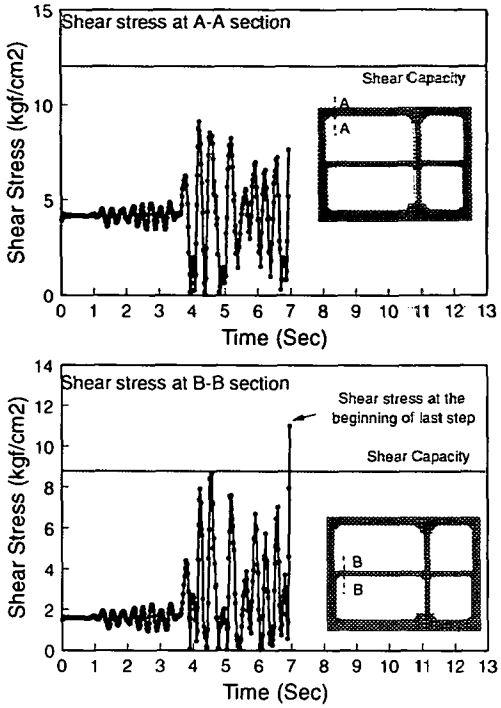

Fig. 28 Shear stress variation in time domain.

It is needed to check the internal stress condition carefully to confirm the mode of failure. **Fig.27** shows the internal shear stresses and the shear deformation of the column. It can be seen through comparison with **Fig.15** that the shear strength induced to the column is hardly affected but merely the induced axial compression is influenced.

The shear stress variations at section A-A and B-B in the upper and middle slabs are shown in **Fig.28**. Section A-A is the point where the slab failed in shear mode in case where only shear reinforcement is enhanced(**Fig.16**). Provided that the up-down motion is cut in computation, the shear stress in section A-A does not reach the failure level(over 15 kgf/cm^2), but the shear stress in section B-B of the middle slab reaches shear capacity (over 9kgf/cm^2). So, the structure would fail in the middle slab as a result of erasing the vertical ground motion in computation.

Even though the vertical ground motion is not a primary cause of the failure, the combination of horizontal and vertical wave may change the dynamic response of the structure including the location of the failure position. The effect of this combination is very complex and needs to be further studied to understand the core of mechanism.

(3) Seismic action characteristics

As stated above, the Kobe wave recorded at Kobe meteorological observatory includes very high horizontal acceleration with short period. In order to study the effect of characteristics of the seismic wave on the underground structures, two kinds of wave are used for the dynamic computation (**Fig.29**).

The first one is an artificial seismic wave produced for Koutouen area, which is based on the earthquake record on solid engineering foundation[12]. The period of this wave is close to the Kobe wave which the authors used while the maximum horizontal acceleration is a little smaller (**Fig.29a**). The second one is the seismic wave recorded at Amagasaki city. It shows medium acceleration level and long period of motion (**Fig.29b**). The maximum acceleration in both horizontal and vertical directions is similar. **Fig.30** shows the inelastic strain representing the damage level in dynamic response. It can be seen that the target underground RC failed under the artificial Koutouenn wave but no failure was brought under the Amakasaki wave.

The deformation profile of RC-soil system when failure occurs is shown in **Fig.31.** This deformation profile is very close to that under the seismic load of Kobe wave (**Fig.8**). The deformation is also concentrated into the upper column, where the failure took place in reality.

The crack pattern at failure is shown in **Fig.32**. The zoom of upper column shows many diagonal shear cracks occurring at this time while only few cracks are introduced at the other parts of the RC frame. This situation is also similar to the original case under the Kobe wave.

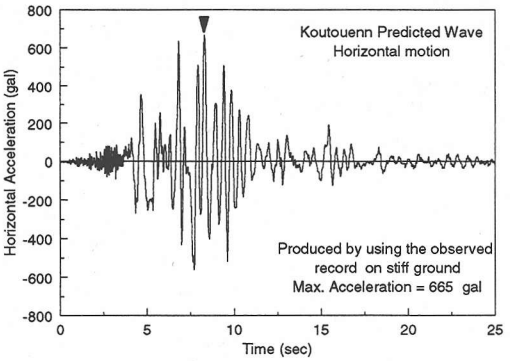

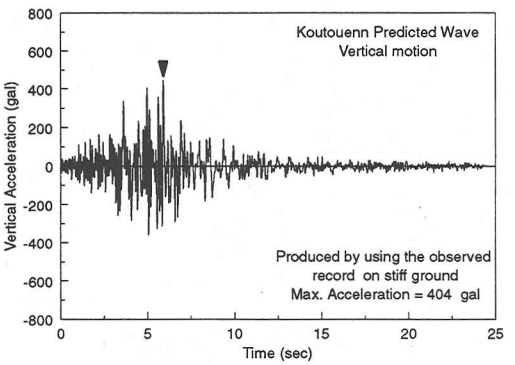

Fig.29a Artificial acceleration profile for Koutouenn area[12].

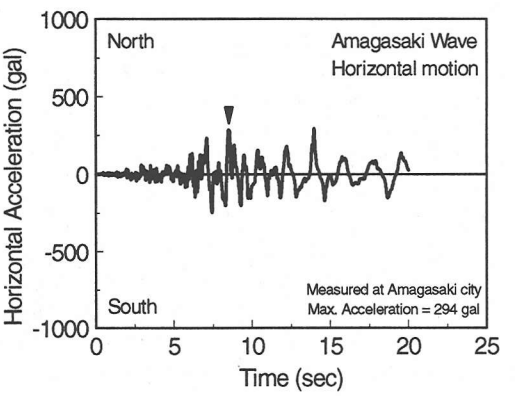

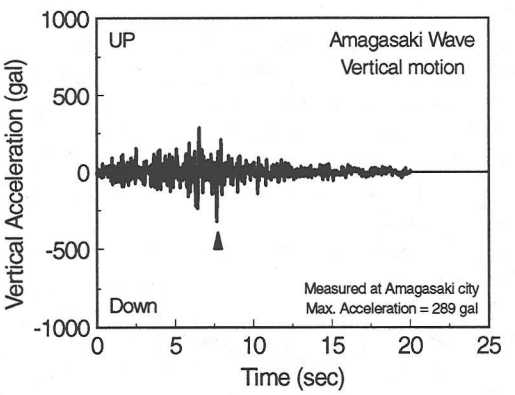

Fig.29b Acceleration records at Amagasaki city.

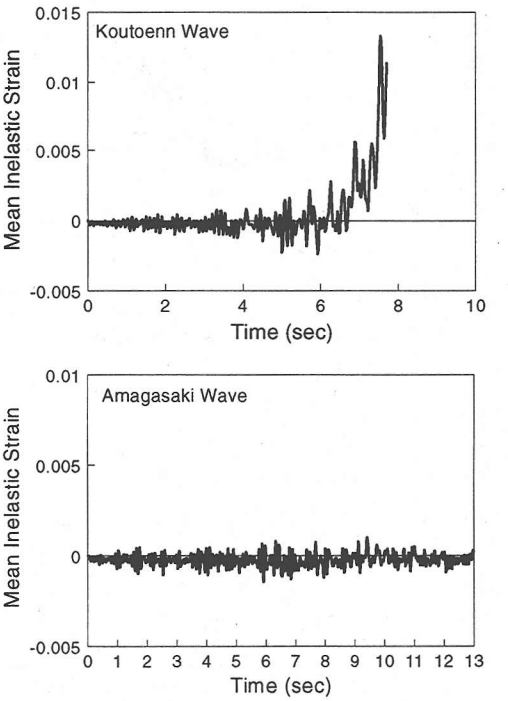

Fig.30 Inelastic strain representing the damage in time domain.

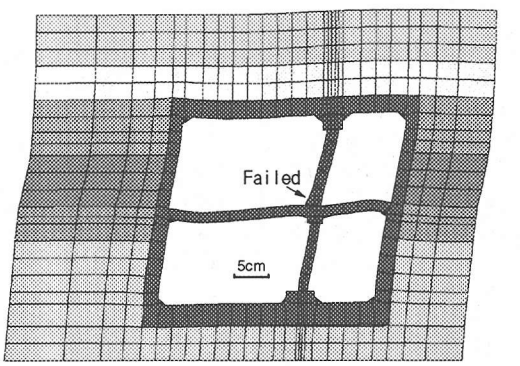

Fig.31 Deformation profile of RC-soil system at failure under Koutouen wave.

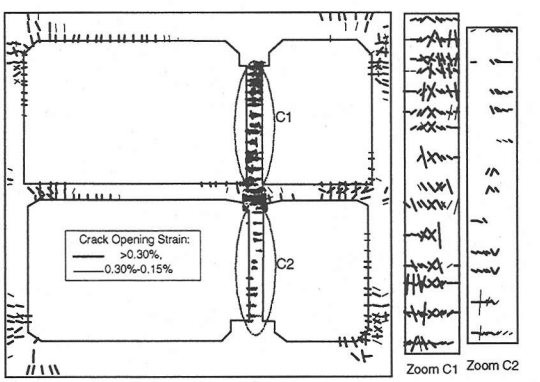

Fig.32 Crack pattern at the failure under Koutouenn wave.

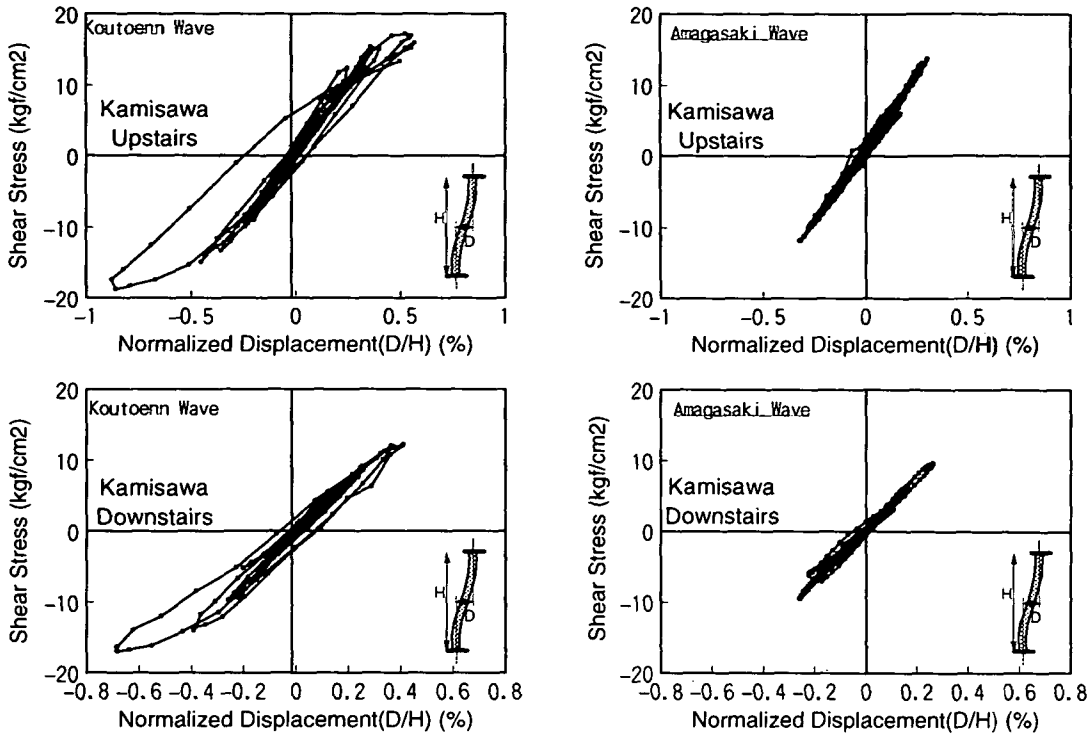

Fig.33 Shear stress-displacement relationship for columns.

The internal shear stresses in the intermediate columns are shown in **Fig.33** for these two cases. Under the seismic load of Koutouen, the shear stress in the upper column comes up to nearly 20 kgf/cm^2, and failed at this time, which is similar to the original case under the Kobe wave (**Fig.10a**). In the case of Amagasaki wave, the shear stress was less than 15 kgf/cm^2, and there is no failure in both of the columns.

Within the limited numbers of input waves, the seismicity with higher acceleration may cause collapse of the middle columns. But, it is not the general case because all the wave characteristics and mechanical properties of both RC and foundation would be influential on the safety. It can be just concluded that overall seismic performance of underground RC must be estimated in consideration of soil and RC nonlinearity under dynamics in time and space.

6. CONCLUSION

In this study, seven cases of dynamic analyses for an underground reinforced concrete box-section damaged in Kobe city were conducted. The group I (**Table 2**), including three cases, was performed for the collapse study with seismic resistant view point.

In group II, the soil profile and the characteristics of the seismic wave have been changed for some trial computation, in order to understand the effect of soil-structure interaction in the dynamic system of underground RC structures.

According to the results of these analyses, we have,

(1) Nonlinear mechanics of reinforced concrete coupled with soil nonlinearity can be a tool for simulating the collapse of underground structure under seismic action and evaluating its performances.

(2) The collapse of subway station is due to the low shear capacity and ductility of the intermediate columns.

(3) Well known and accepted strategy that an increase in shear capacity enhances ductility and seismic resistance is confirmed to be effective for design of underground RC, too.

(4) The soil profile affects the damage level and failure location. Softer foundation may cause larger shear damage.

(5) Combination of horizontal and vertical component of seismic action is a factor which affects the location of failure of existing underground RC.

(6) Seismic waves from different sources give similar dynamic response if the wave has similar period and maximum acceleration. Further discussion is needed on the characteristics of earthquake wave.

ACKNOWLEDGMENT : The authors appreciate technical advises by Dr. A. Shawky, Cairo University, and kind offer of the seismic acceleration diagram by Dr. Hajime Ouchi, Ohbayashi Corporation.

REFERENCES

1) Samata, S., Nagamitsu N., Yamamoto, K. and Mori, S. : A study on a failure mechanism of subway station analyzed by a non-linear seismic deformation method, *Proceedings of Technical Conference on the Great Hanshin- Awaji Earthquake, JSCE*, Tokyo, pp.231-238, 1996.
2) Tajiri, M., Samata, S., Siba, Y., Sakashita, K. and Watanabe, K. : An analytical study on failure mechanism of a subway station damaged by the 1995 Hyogoken-Nanbe earthquake, *Proceedings of Technical Conference on the Great Hanshin-Awaji Earthquake*, JSCE, Tokyo, pp.239-246, 1996.
3) Okamura, H. and Maekawa, K.: *Nonlinear Analysis and Constitutive Models of Reinforced Concrete*, Gihodo, Tokyo, 1991.
4) Okamura, H. and Maekawa, K. : Reinforced concrete design and size effect in structural nonlinearity, invited, *Proceeding of JCI International Workshop: Size Effect in Concrete Structures*, Sendai, Japan, pp.1-20, 1993.
5) Collins, M.P. and Mitchell, D. : *Prestressed Concrete Structures*, PRENTICE HALL, Englewood Cliffs, New Jersey 07632, pp.345, 1991.
6) Shawky, A. and Maekawa, K. : Nonlinear dynamic analysis for underground reinforced concrete structures, *East Asian-Pacific Conference on Structural Engineering and Construction*, EASEC-5, Australia, July, 1995.
7) Ohsaki, Y. : Some notes on Masing's law and nonlinear response of soil deposits, *Journal of the Faculty of Eng. (B), The University of Tokyo*, Vol. XXXV, No. 4, 1980.
8) Shawky, A. and Maekawa, K. : Computational approach to path-dependent nonlinear RC/soil Interaction, *J. Material, Concrete. Struct., Pavements*, JSCE, No.532/V-30, pp.197-207, Feb, 1996.
9) Tajiri, M., Samata, S., Matsuda, T. and Ouchi, H. : A study on the damage of underground railway structure during the Great Hanshin Earthquake, *Proceedings of Technical Conference on the Great Hanshin- Awaji Earthquake*, JSCE, Tokyo, pp.255-262, 1996.
10) JSCE, *Standard specification for design and construction of concrete structure*, pert I(Design), 1st ed, Tokyo, 1986.
11) Shawky, A. and Maekawa, K. : Collapse mechanism of underground RC structures during Hanshin Great Earthquake, *Cairo first International Conference on Concrete Structures*, 1996.
12) Ouchi, H., Ejiri, J., Matsumoto, N. and Matsuoka, Y. : A study on the Shinkansen viaduct damage during the Great Hanshin Earthquake and seismic performance of retrofitted structure, *Proceedings of Technical Conference on the Great Hanshin-Awaji Earthquake*, JSCE, Tokyo, pp.305-312, 1996.

(Received August 5, 1996)

地震作用を受ける地中鉄筋コンクリートの破壊解析

Xuehui AN・前川宏一

本研究は地中鉄筋コンクリート構造の破壊解析を提示し,経路依存性を考慮した材料構成モデルに基づき,地中構造の破壊機構について論ずるものである.考慮した非線形性は鉄筋コンクリート,地盤材料および地盤構造間の応力伝達機構である.主として鉛直荷重を支える部材のせん断破壊に着目し,破壊に及ぼす地盤の非線形性,地震入力の違い及び鉛直成分の有無について検討を行った.保有する耐震性能は地盤と構造自体の非線形性を共に考慮しなければならないことが確認された.